Accurate Formula for the Macroscopic Polarization of Strongly Correlated Materials

Ryan Requist*,[†][iD] and E. K. U. Gross[†,‡]

[†]Max Planck Institute of Microstructure Physics, Weinberg 2, 06114 Halle, Germany

[‡]Fritz Haber Center for Molecular Dynamics, Institute of Chemistry, The Hebrew University of Jerusalem, Jerusalem 91904, Israel

S *Supporting Information*

ABSTRACT: The many-body Berry phase formula for macroscopic polarization is approximated by a sum of natural orbital geometric phases with fractional occupation numbers accounting for the dominant correlation effects. This formula accurately reproduces the exact polarization in the Rice−Mele−Hubbard model across the band insulator−Mott insulator transition. A similar formula based on a reduced Berry curvature accurately predicts the interaction-induced quenching of Thouless topological charge pumping.
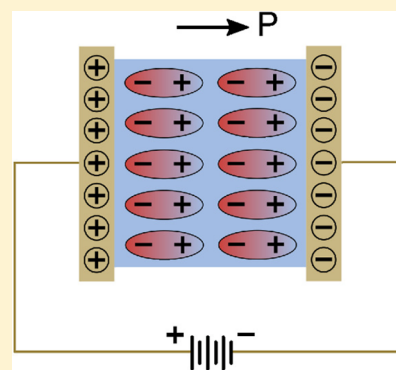
Macroscopic polarization is a fundamental property of dielectric materials from which permittivity and piezoelectric tensors and several other physical variables can be derived. A solid can polarize spontaneously, as occurs in ferroelectrics, or in response to an applied electric field, strain, and other external perturbation.[1] Ferroelectric perovskite oxides are an interesting class of materials for photovoltaic applications because their electric polarization promotes charge separation.[2] Ferroelectric domains are thought to contribute to the high performance of hybrid perovskite solar cells,[3,4] and light-enhanced piezoelectricity has been observed in lead halide perovskites.[5]

A satisfactory theory of bulk macroscopic polarization was formulated only relatively recently[6−9] after the realization that a change in polarization, which is what is usually measured in experiment, can be related to the net adiabatic charge transport;[6] see ref 10 for a lucid account. King-Smith and Vanderbilt derived the following formula for the change induced by adiabatically varying an arbitrary Hamiltonian parameter λ[8]

$$\Delta \mathbf{P} = -e \int_0^1 d\lambda \int_{BZ} \frac{d^3k}{(2\pi)^3} 2 \, \mathrm{Im} \sum_n^{occ} \langle \nabla_{\mathbf{k}} u_{n\mathbf{k}} | \partial_\lambda u_{n\mathbf{k}} \rangle \quad (1)$$

where $u_{n\mathbf{k}}$ is the periodic part of the Bloch state $\phi_{n\mathbf{k}}$. The k integral is over the Brillouin zone, and the sum is over occupied bands. The integrand contains a mixed $(\mathbf{k}, \lambda)$ Berry curvature $B_{\mathbf{k}\lambda} = 2 \, \mathrm{Im} \sum_n \langle \nabla_{\mathbf{k}} u_{n\mathbf{k}} | \partial_\lambda u_{n\mathbf{k}} \rangle$,[11] which also appears in Thouless charge pumping.[12]

The change in polarization in the direction of a lattice vector $\mathbf{R}_\alpha$ can be expressed as a Berry phase,[8] e.g.

$$\Delta P_3 = -\frac{e}{(2\pi)^3} \sum_n^{occ} \int dk_1 \, dk_2 \int_0^{|\mathbf{G}_3|} \mathrm{i} \langle u_{n\mathbf{k}} | \partial_{k_3} u_{n\mathbf{k}} \rangle \, dk_3 |_{\lambda=0}^{\lambda=1} \quad (2)$$

where $\Delta P_3 = \frac{1}{2\pi} \mathbf{G}_3 \cdot \Delta \mathbf{P}$ and the (k_1, k_2) integral is taken over the parallelogram spanned by the reciprocal lattice vectors $\mathbf{G}_1$ and $\mathbf{G}_2$. The geometric phase of a Bloch state on a path traversing the Brillouin zone was introduced by Zak and related to Wyckoff positions.[13,14]

The King-Smith−Vanderbilt formula is exact for non-interacting electrons and has given good results for ferro-electric perovskites and other materials.[15−21] However, if the Bloch states are chosen to be the Kohn−Sham orbitals from a density functional theory (DFT) calculation, as is usually done, the formula is not guaranteed to yield the exact polarization even if the exact exchange−correlation potential is used.[22] The King-Smith−Vanderbilt formula may give incorrect results in strongly correlated materials, and if the single-particle orbitals are chosen to be the Kohn−Sham orbitals, then it is ill-defined for any insulator whose Kohn−Sham system is metallic.[23] On the other hand, if the Bloch states are obtained from an exact calculation in current DFT,[24] then an adaptation of the arguments in ref 25 suggests that eq 1 might give the correct $\Delta \mathbf{P}$.

Ortiz and Martin[9] generalized the King-Smith−Vanderbilt formula to correlated many-body systems using twisted boundary conditions, a concept that has been used to analyze

TH-2018-36

the insulating state of matter,[26] the integer quantum Hall effect,[27−29] and topological charge pumping.[12,30] For one-dimensional systems, the Ortiz−Martin formula reads

$$\Delta P = -\frac{e}{2\pi} \lim_{\substack{N,L\to\infty \\ N/L=\text{const.}}} \int_0^{2\pi/L} i\langle \Phi_0|\partial_k\Phi_0\rangle \, dk|_{\lambda=0}^{\lambda=1} \quad (3)$$

where N is the number of electrons in a supercell of length L. The many-body state $\Phi_0 = \Phi_0(x_1, ..., x_N)$ is the ground state of the "twisted" Hamiltonian

$$\hat{H}(k, \lambda) = \sum_{i=1}^{N} \frac{(p_i + \hbar k)^2}{2m} + \sum_{\langle ij\rangle} \frac{e^2}{|r_i - r_j|} + \hat{V}_{\text{ext}}(\lambda) \quad (4)$$

where $\hat{V}_{\text{ext}}(\lambda)$ includes the electron−ion interaction and any other external potentials and the parameter k generates an effective magnetic flux that takes on the role of the twisted boundary conditions. The twisted boundary conditions on the ground state of the original Hamiltonian $\hat{H}'$ are $\Phi_0'(x_1, ..., x_i + L, ..., x_N) = e^{ikL}\Phi_0'(x_1, ..., x_i, ..., x_N)$ for all i. The ground state of the twisted Hamiltonian $\hat{H} = \hat{U}^\dagger\hat{H}'\hat{U}$ with $\hat{U} = e^{ik(\hat{x}_1 + \hat{x}_2 + \cdots + \hat{x}_N)}$ is related to the original ground state by $|\Phi_0\rangle = \hat{U} \,| \Phi_0'\rangle$.

The main result that we report here is a geometric phase formula for the macroscopic polarization that maintains the simplicity and utility of the King-Smith−Vanderbilt formula while capturing the most important correlations in the Ortiz−Martin result. The reduced formula is

$$\Delta \mathbf{P}_{\text{red}} = -e \int_0^1 d\lambda \int_{\text{BZ}} \frac{d^3k}{(2\pi)^3} 2\,\text{Im} \sum_{n=1}^{\infty} \langle \nabla_\mathbf{k} v_{n\mathbf{k}}|\partial_\lambda v_{n\mathbf{k}}\rangle \quad (5)$$

where $v_{n\mathbf{k}}(\mathbf{r}) = \sqrt{f_{n\mathbf{k}}}\, e^{i\zeta_{n\mathbf{k}}} u_{n\mathbf{k}}(\mathbf{r})$ is the periodic part of the natural Bloch state $\psi_{n\mathbf{k}}(\mathbf{r}) = e^{i\mathbf{k}\cdot\mathbf{r}} v_{n\mathbf{k}}(\mathbf{r})$; $v_{n\mathbf{k}}(\mathbf{r})$ is analogous to $u_{n\mathbf{k}}(\mathbf{r})$ in eq 1. The natural Bloch orbitals $\phi_{n\mathbf{k}}(\mathbf{r}) = e^{i\mathbf{k}\cdot\mathbf{r}} u_{n\mathbf{k}}(\mathbf{r})$ and occupation numbers $f_{n\mathbf{k}}$ are eigenfunctions and eigenvalues of the one-body reduced density matrix (rdm) $\rho_1(\mathbf{r}\sigma, \mathbf{r}'\sigma')$,[31] and $\zeta_{n\mathbf{k}}$ is a crucial additional phase variable that determines the gauge of $\psi_{n\mathbf{k}}(\mathbf{r})$. Given any gauge choice for the natural Bloch orbitals $\phi_{n\mathbf{k}}(\mathbf{r})$, the ground state $\zeta_{n\mathbf{k}}$ can be determined from the stationary conditions $\partial E/\partial \zeta_{n\mathbf{k}} = 0$, where $E = \langle \Phi'|\hat{H}'|\Phi'\rangle$ and $|\Phi'\rangle = \exp[i\sum_{n\mathbf{k}} \zeta_{n\mathbf{k}}\hat{f}_{n\mathbf{k}}]|\Phi^{\text{Ansatz}}\rangle$. Here, $\hat{f}_{n\mathbf{k}} = b_{n\mathbf{k}}^\dagger b_{n\mathbf{k}}$ is the number operator for $\phi_{n\mathbf{k}}(\mathbf{r})$ and

$$|\Phi^{\text{Ansatz}}\rangle = \sum_{n_1\mathbf{k}_1, n_2\mathbf{k}_2, ..., n_N\mathbf{k}_N} c_{n_1\mathbf{k}_1, n_2\mathbf{k}_2, ..., n_N\mathbf{k}_N} |\phi_{n_1\mathbf{k}_1}\phi_{n_2\mathbf{k}_2}\cdots\phi_{n_N\mathbf{k}_N}\rangle \quad (6)$$

is an Ansatz for the wave function as a superposition of Slater determinants of natural Bloch orbitals. It follows from this definition that if we make a gauge transformation $\phi_{n\mathbf{k}}(\mathbf{r}) \to e^{i\theta_{n\mathbf{k}}}\phi_{n\mathbf{k}}(\mathbf{r})$, the $\zeta_{n\mathbf{k}}$ transform as $\zeta_{n\mathbf{k}} \to \zeta_{n\mathbf{k}} - \theta_{n\mathbf{k}}$. Hence, the phases of $\psi_{n\mathbf{k}}(\mathbf{r})$ and $v_{n\mathbf{k}}(\mathbf{r})$ are invariant under such a transformation, and any geometric or topological quantity constructed from them, including $\Delta\mathbf{P}_{\text{red}}$ in eq 5, is gauge-invariant (see later for further discussion).

Equation 5 expresses the change in polarization as a sum of single-particle band contributions, like the King-Smith−Vanderbilt formula, but uses natural orbitals instead of Kohn−Sham orbitals. The natural orbitals are intrinsic variables of the many-body wave function rather than eigenstates of an effective mean-field Hamiltonian. Because the natural Bloch state $\psi_{n\mathbf{k}}$ contains the factor $f_{n\mathbf{k}}$ and $0 \leq f_{n\mathbf{k}} \leq 1$ as a result of quantum and thermal fluctuations, each valence band contribution is diminished with respect to the non-interacting case, and there are nonvanishing conduction band

contributions; here, "valence" denotes bands with occupation numbers $f_{n\mathbf{k}} > 1/2$, and "conduction" denotes bands with occupation numbers $f_{n\mathbf{k}} < 1/2$ (see later for a more precise definition). Equation 5 rests on the assumption that the sum of the natural orbital geometric phases is a good approximation to the geometric phase of the full correlated many-body state. Reasons for the accuracy of this approximation will be discussed below after our numerical results are reported.

Polarization in the Rice−Mele−Hubbard Model. Resta and Sorella[32] applied the Ortiz−Martin formula to the Rice−Mele−Hubbard model, also known as the ionic Hubbard model,[33,34] which is a model obtained by adding Hubbard interactions to the Su−Schrieffer−Heeger[35] or Rice−Mele[36] models. It exhibits a quantum phase transition between band insulating and Mott insulating phases at a critical value of the Hubbard parameter U_c, with the many-body geometric phase providing an order parameter for the transition.[32] Subsequent works have used geometric phases to further characterize quantum phase transitions.[37−41] Recently, higher-order cumulants and the total distribution of the polarization have been calculated for the noninteracting Rice−Mele model.[42]

The Hamiltonian of the Rice−Mele−Hubbard model can be written as (see, e.g., ref 43)

$$\hat{H} = -t_1 \sum_{i\sigma} c_{i\sigma}^\dagger c_{i\sigma} \otimes \hat{\tau}_x - t_2 \sum_{i\sigma}\left(c_{i\sigma}^\dagger c_{i+1\sigma} \otimes \frac{\hat{\tau}_-}{2} + \text{H.c.}\right)$$
$$+ \Delta \sum_{i\sigma} c_{i\sigma}^\dagger c_{i\sigma} \otimes \hat{\tau}_z + U \sum_i \hat{n}_{i\uparrow}\hat{n}_{i\downarrow} \otimes \hat{I} \quad (7)$$

where $\hat{\vec{\tau}}$ are the Pauli matrices in the (A, B) sublattice basis, $\hat{\tau}_\pm = \hat{\tau}_x \pm i\hat{\tau}_y$, and $t_{1,2} = t_0 \mp 2g\xi$, with $g = 10$ eV/a denoting the electron−phonon coupling and ξ the displacement of B with respect to A. As illustrated in Figure 1, there are two atoms in the primitive cell; A represents a cation and B an anion. The lattice constant is a.
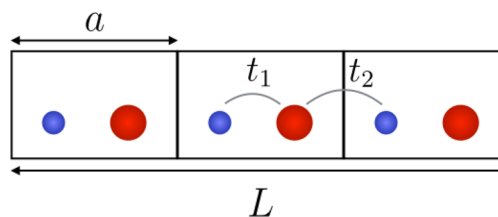

Figure 1. Schematic of the Rice−Mele−Hubbard model with one cation (blue) and one anion (red) in the primitive cell.

Before testing eq 5, we calculate the exact ΔP using the Ortiz−Martin formula. First, we choose a supercell of length $L = Ma$, $M \in \mathbb{Z}$, and define the lattice analogue of the twisted Hamiltonian in eq 4 by making the replacement

$$t_2\left(c_{M\sigma}^\dagger c_{1\sigma} \otimes \frac{\hat{\tau}_-}{2} + \text{H.c.}\right) \to t_2\left(e^{i\alpha} c_{M\sigma}^\dagger c_{1\sigma} \otimes \frac{\hat{\tau}_-}{2} + \text{H.c.}\right)$$

in eq 7. Second, we calculate the ground state $|\Phi_0(\alpha, M)\rangle$ for twist angles $\alpha \in [0, 2\pi]$ using the Lanczos algorithm. Third, we evaluate the geometric phase

$$\gamma(\xi, M) = \int_0^{2\pi} i\langle\Phi_0|\partial_\alpha\Phi_0\rangle \, d\alpha \quad (8)$$

One can use the discretized Berry phase formula with the boundary condition $|\Phi_0(2\pi, M)\rangle = e^{-i2\pi(\hat{x}_1 + ... + \hat{x}_N)/L}|\Phi_0(0, M)\rangle$.

Finally, we calculate $\Delta P(M) = -(e/2\pi)[\gamma(\xi_2, M) - \gamma(\xi_1, M)]$ for an adiabatic variation from ξ_1 to ξ_2 for a series of M values and extrapolate to the thermodynamic limit to obtain $\Delta P = \lim_{M\to\infty} \Delta P(M)$. The many-body geometric phase also gives the polarization $P = -(e/2\pi)\gamma$, which is, however, only defined modulo e because γ is only defined up to a multiple of 2π.

Given any method for obtaining the natural Bloch states ψ_{nk}, eq 5 allows one to circumvent the computationally intensive calculation of the many-body wave function. Because such a method is not yet available, we will use the following procedure to reconstruct ψ_{nk} from the information contained in $|\Phi_0(\alpha, M)\rangle$. From the numerically exact ground state $|\Phi_0(\alpha, M)\rangle$ of a supercell of length $L = Ma$, obtained as described above, we calculate the natural orbitals $\phi_n(\alpha, M)$, occupation numbers $f_n(\alpha, M)$, and phases $\zeta_n(\alpha, M)$ as functions of $\alpha = [0, 2\pi]$. If the primitive cell has z orbitals, there will be zM natural orbitals in the supercell (the Rice–Mele–Hubbard has two spin-degenerate bands; therefore, $z = 4$). Reexpressing the α-dependent $\{\phi_n, f_n, \zeta_n\}$ as functions of the supercell quasimomentum $k = \frac{\alpha - \pi}{L} \in \left[-\frac{\pi}{L}, \frac{\pi}{L}\right]$ defines natural Bloch orbitals $\phi_{nk}(M) = \phi_n(kL + \pi, M)$ and natural occupation number bands $f_{nk}(M) = f_n(kL + \pi, M)$ that live in the supercell Brillouin zone. Since the normal Brillouin zone of the crystal is M times larger than the supercell Brillouin zone, we obtain z natural Bloch states, $\psi_{nk}(M)$, by unfolding $\sqrt{f_{nk}(M)} \exp[i\zeta_{nk}(M)]\phi_{nk}(M)$ to the normal Brillouin zone $k \in \left[-\frac{\pi}{a}, \frac{\pi}{a}\right]$; see later in the text for more detail on the unfolding procedure. Finally, we define the M-dependent reduced polarization

$$\Delta P_{\rm red}(M) = -\frac{e}{2\pi} \sum_{n=1}^{z} \left[\int_{-\pi/a}^{\pi/a} i\langle v_n|\partial_k v_n\rangle \, dk \right]_{\xi_1}^{\xi_2} \quad (9)$$

which converges to eq 5 in the thermodynamic limit, i.e., $\Delta P_{\rm red} = \lim_{M\to\infty} \Delta P_{\rm red}(M)$. The sum runs over the z natural occupation number bands in the normal Brillouin zone.

Defining the natural orbital geometric phases

$$\gamma_n(\xi) = \int_{-\pi/a}^{\pi/a} i\langle v_n|\partial_k v_n\rangle \, dk \quad (10)$$

it is seen that eq 9 depends on the sum $\sum_n \gamma_n$, which we shall refer to as the (one-body) reduced geometric phase $\gamma_{\rm red}$ because it approximates the many-body geometric phase in eq 8 with the variables from reduced density matrices.

Because the one-body part of the Hamiltonian, $\hat{H}_0$, has translational symmetry, i.e., $[\hat{H}_0, \hat{T}_a] = 0$, where $\hat{T}_a$ in eq 9 is the displacement operator, its eigenstates are readily obtained by diagonalizing the k-space Hamiltonian

$$\hat{H}_0(k) = \langle k\sigma|\hat{H}_0|k\sigma\rangle = \vec{h}_0(k\sigma)\cdot\hat{\vec{\tau}} \quad (11)$$

where $\vec{h}_0(k\sigma) = \{-t_1 - t_2 \cos k, -t_2 \sin k, \Delta\}$. Here, the plane waves $|k\sigma\rangle = \frac{1}{\sqrt{M}} \sum_{l=1}^{M} e^{ikl}c_{l\sigma}^{\dagger}|0\rangle$ are defined for periodic boundary conditions and $k = 2\pi m/M$; $m = 0, 1, ..., M - 1$. The eigenfunctions of $\hat{H}_0(k)$ define the periodic parts $|u_{nk}\rangle$ of the Bloch states $|\chi_{nk\sigma}\rangle = |u_{nk}\rangle|k\sigma\rangle$.

When the artificial gauge potential implied by α is turned on, the states maintain their Bloch form, but the allowed values of k shift to $k = (2\pi m + \alpha)/M$. Hubbard interactions do not break overall translational symmetry; therefore, the many-body

eigenstates can be labeled by the total quasimomentum K. Because the Hamiltonian commutes with $\hat{S}^2$ and $\hat{S}_z$, we also have the quantum numbers S and S_z. For example, only configurations whose occupied Bloch states $\{|\chi_{n,k_i,\sigma_i}\rangle\}$ satisfy $\sum_{i=1}^{N} k_i = K$ and $\sum_{i=1}^{N} \sigma_i/2 = S_z$ contribute to the many-body eigenstate.

The results presented below were obtained for the Rice–Mele–Hubbard model with $N = 6$ and $M = 3$ ($L = 3a$), corresponding to six electrons in six sites. The ground state is a spin singlet with quantum numbers $K = 0$, $S = 0$, and $S_z = 0$. The dimension of the $S_z = 0$ Hilbert space is 400, which reduces to 136 with $K = 0$. The SNEG package was used to set up the Hamiltonian.[44]

After calculating the ground state $|\Phi_0\rangle$, the natural Bloch orbitals and occupation numbers were readily obtained by diagonalizing the one-body rdm

$$\rho_{aa'}(k\sigma) = \langle\Phi_0|\hat{c}_{a'k\sigma}^{\dagger}\hat{c}_{ak\sigma}|\Phi_0\rangle \quad (12)$$

where $\hat{c}_{ak\sigma}^{\dagger}$ is the creation operator for the sublattice Bloch state $\chi_{ak\sigma} = |a\rangle|k\sigma\rangle$, where $a = A, B$. Because the one-body rdm commutes with $\hat{T}_a$ in eq 9 and $\hat{S}_z$, it is diagonal in k and σ.

Figure 2 shows the occupation number band structure. The three largest spin-independent occupation numbers f_1, f_2, and
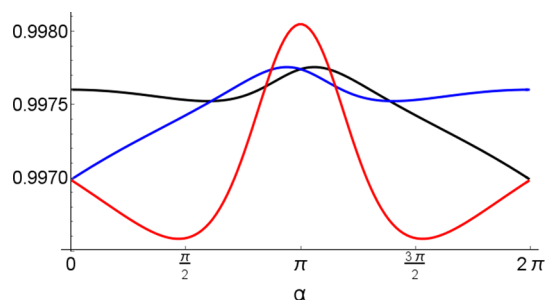

Figure 2. Three largest occupation numbers $f_{n\sigma}$ for hopping $t_0 = 3.5$ eV, sublattice displacement $\xi = 0.0140a$, staggered potential $\Delta = 2.0$ eV, and Hubbard interaction $U = 0.8t_0$.

f_3 are plotted as functions of α; $f_n \equiv f_{n\sigma}$. There are additionally three small occupation numbers, f_4, f_5, and f_6 that, however, are not independent variables due to the conditions $f_1 + f_6 = 1$, $f_2 + f_5 = 1$, and $f_3 + f_4 = 1$ (see the Supporting Information). Because the occupation numbers tend to cluster near 0 and 1, there are inevitably frequent crossings as α is varied. To identify the individual bands as smooth functions of α, we used a maximum overlap criterion referring to the natural Bloch orbitals at adjacent α points.

The occupation numbers f_1, f_2, and f_3 are branches of a single multivalued function. The f_n can be matched smoothly to one another at the boundaries of the α domain $[0, 2\pi]$, e.g., $f_1(2\pi) = f_3(0)$, $f_3(2\pi) = f_2(0)$, and $f_2(2\pi) = f_1(0)$. By extending the domain to $[0, 6\pi]$, the occupation numbers f_1, f_2, and f_3 can be "unfolded" to form a single strongly occupied valence band $f(\alpha)$ in the normal Brillouin zone, as shown in Figure 3. Similarly, f_4, f_5, and f_6 form a single weakly occupied conduction band. New definitions need to be introduced for the terms "valence band" and "conduction band" because natural Bloch orbitals do not have definite energy eigenvalues. In the N-electron case, let $f_{nk}(U)$ and $\phi_{nk}(U)$ be the occupation number bands and natural Bloch orbitals as functions of the interaction strength U. If we turn U down close to zero, we will have N nearly fully occupied bands
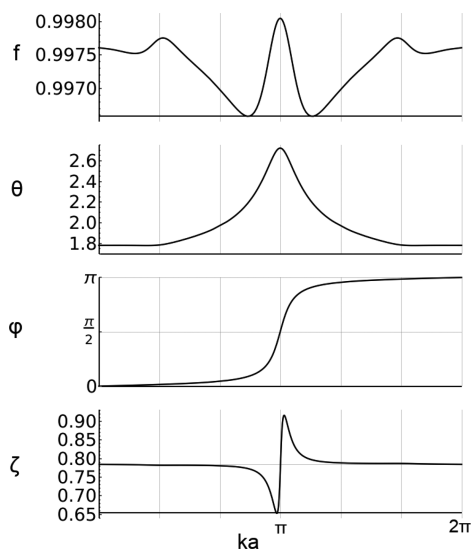
Figure 3. Unfolded natural orbital variables f, θ, φ, and ζ in the normal Brillouin zone for the same parameters as those in Figure 2.

$[f_{nk}(0^+) \approx 1]$ and generally an infinite number of very weakly occupied bands $[f_{nk}(0^+) \approx 0]$. As we turn U back up, the N nearly fully occupied $f_{nk}(U)$ will evolve smoothly into N occupation number bands that tend to have $f_{nk}(U) > \frac{1}{2}$; we refer to these strongly occupied bands as "valence" bands. At the same time, some of the $f_{nk}(U)$ that were essentially unoccupied for very small U will acquire significant occupancy but will still tend to have $f_{nk}(U) < \frac{1}{2}$; we refer to these weakly occupied bands as "conduction" bands. These definitions will need to be extended in the case of occupation number band degeneracies.

In the sublattice basis, the natural Bloch orbitals are

$$\phi_n(l) = \begin{cases} \dfrac{e^{ik_n l}}{\sqrt{3}} \begin{pmatrix} \cos(\theta_n/2) \\ \sin(\theta_n/2)e^{i\varphi_n} \end{pmatrix} & n = 1, 2, 3 \\[2em] \dfrac{e^{ik_n l}}{\sqrt{3}} \begin{pmatrix} \sin(\theta_n/2) \\ -\cos(\theta_n/2)e^{i\varphi_n} \end{pmatrix} & n = 4, 5, 6 \end{cases}$$

(13)

where $l = 0, 1, 2$ labels the cell within the supercell and $k_1 = k_6 = \frac{\alpha}{3}$, $k_2 = k_5 = -\frac{2\pi}{3} + \frac{\alpha}{3}$, and $k_3 = k_4 = \frac{2\pi}{3} + \frac{\alpha}{3}$. The natural Bloch orbitals match up smoothly at the boundaries of the interval $[0, 2\pi]$, in direct correspondence with the occupation numbers. Unfolding the natural Bloch orbitals defines the functions $\theta(\alpha)$ and $\varphi(\alpha)$ shown in Figure 3.

The last quantities that we need are the ζ_n. These phases could be determined from the variational principle, as described earlier in the text, but because this is impractical in problems with large Hilbert spaces, we propose the following alternative route to calculate them. First, calculate the set of two-body rdm elements $\rho_{ijkl}^{\rho\sigma\tau\upsilon} = \langle \Phi_0 | \hat{b}_{l\upsilon}^\dagger \hat{b}_{k\tau}^\dagger \hat{b}_{i\rho} \hat{b}_{j\sigma} | \Phi_0 \rangle$, where $\hat{b}_{j\sigma}^\dagger$ is the creation operator for natural Bloch orbital $\phi_{j\sigma}$. Then, we use the Moore–Penrose pseudoinverse[45] to solve the overdetermined equations $\zeta_{i\rho} + \zeta_{j\sigma} - \zeta_{k\tau} - \zeta_{l\upsilon} = \mathrm{Arg}\,\rho_{ijkl}^{\rho\sigma\tau\upsilon}$. It is clear from this definition that the $\zeta_{j\sigma}$ obey the gauge transformation rule $\zeta_{j\sigma} \to \zeta_{j\sigma} - \theta_{j\sigma}$ when the phase of a natural Bloch orbital is changed according to $\phi_{j\sigma} \to e^{i\theta_{j\sigma}}\phi_{j\sigma}$.

Thus, the natural Bloch state $\psi_{j\sigma} = \sqrt{f_{j\sigma}}\,e^{i\zeta_{j\sigma}}\phi_{j\sigma}$ is gauge-invariant.

For $M = 3$, a simplification is possible because in this case the only nonzero elements of the type $\rho_{iijj}^{\uparrow\downarrow\uparrow\downarrow}$ are $\rho_{1166}^{\uparrow\downarrow\uparrow\downarrow}$, $\rho_{2255}^{\uparrow\downarrow\uparrow\downarrow}$, and $\rho_{3344}^{\uparrow\downarrow\uparrow\downarrow}$ and their Hermitian conjugates. These elements are sufficient to determine $\zeta_1 - \zeta_6$, $\zeta_2 - \zeta_5$, and $\zeta_3 - \zeta_4$. Due to particle–hole symmetry (Supporting Information section S3), the reduced geometric phase γ_{red} only depends on these combinations of ζ_n variables. The unfolded $\zeta(\alpha)$ is shown in Figure 3.

The coefficients of the many-body wave function in a fixed natural Bloch orbital basis also connect up as functions of α, and ζ_n control relative phases between the configurations. Changing the ζ_n changes the n-body correlation functions, e.g., the probability of double occupancy $D_a = \langle \Phi_0 | \hat{n}_{a\uparrow} \hat{n}_{a\downarrow} | \Phi_0 \rangle$ on sublattice $a = A, B$ and, therefore affects the energy.[46]

In terms of the unfolded functions $f(k)$, $\theta(k)$, $\varphi(k)$, and $\zeta(k)$ with $k = \frac{\alpha - \pi}{L}$, the periodic part $|v_{nk}\rangle$ of the natural Bloch state $|\psi_{nk}\rangle = |v_{nk}\rangle|k\sigma\rangle$ can be parametrized as

$$|v_{1k}\rangle = \sqrt{f}\,e^{i\zeta} \begin{pmatrix} \cos(\theta/2) \\ \sin(\theta/2)e^{i\varphi + ikr_B} \end{pmatrix}$$

$$|v_{2k}\rangle = \sqrt{1-f}\,e^{-i\zeta} \begin{pmatrix} \sin(\theta/2) \\ -\cos(\theta/2)e^{i\varphi + ikr_B} \end{pmatrix}$$

(14)

for the valence and conduction bands, respectively. Here $r_B = a/2$ is the coordinate of the ion at site B ($r_A \equiv 0$).

We now have the ingredients needed to calculate ΔP_{red} in eq 9. As all of the information is contained in the geometric phases, we shall simply compare the reduced geometric phase γ_{red} with the exact geometric phase γ. In the noninteracting case, the valence band Wannier function center $\langle \hat{r} \rangle$ is related to $\gamma/2$ by $\langle \hat{r} \rangle/a = (\gamma/2)/(2\pi)$; the factor of $1/2$ accounts for spin degeneracy. Figure 4 shows $\gamma/2$ and $\gamma_{\mathrm{red}}/2$ as functions of U for
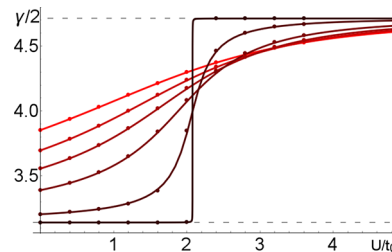

Figure 4. Exact (lines) and reduced (points) geometric phases for sublattice displacement $\xi = (5.00 \times 10^{-6}, 0.0035, 0.0140, 0.0245, 0.0350, 0.0500)a$ [dark to light]. Dashed lines show π and $3\pi/2$.

several values of the sublattice displacement ξ. For $\xi = 5 \times 10^{-6}a$, corresponding to an almost centrosymmetric lattice, there is an almost discontinuous jump of π in γ as U passes through U_c.[32] This implies a sudden change of $e/2$ in the polarization at the band insulator–Mott insulator transition. The reduced geometric phase is an accurate approximation to the exact geometric phase, with a maximum error of $\lesssim 1\%$, throughout the range of parameters in Figure 4. The calculations were performed with between 64 and 96 α points. The data points for $\xi = 5 \times 10^{-6}a$ were obtained for $|v_{nk}\rangle$ without the $\sqrt{f_n}\,e^{i\zeta_n}$ factors.

The accuracy of eq 5 is partially a consequence of pure-state N-representability constraints,[47−49] which are nontrivial (in)-equalities that the occupation numbers must satisfy in order to be consistent with an N-electron pure state. In some two- and three-electron systems, the exact saturation of these constraints is known to make the many-body geometric phase reduce exactly to the sum of natural orbital geometric phases. This occurs in the two-site Hubbard model[46] and three-site Hubbard ring[50] as a consequence of the Löwdin−Shull[51] and Borland−Dennis conditions.[52] To our knowledge, the N-representability constraints are not yet known for the case of interest here, i.e., $N = 6$ and Hilbert space dimension $d = 12$, although a general algorithm for determining them has been introduced.[48,49] If the inequality constraints are found to be nearly saturated, i.e., if the occupation numbers are quasipinned,[53−55] it would suggest that the reduced geometric phase deviates from the full geometric phase by a correspondingly small quantity that vanishes as the occupation numbers approach the relevant boundary of their allowed region. Natural orbital geometric phases are themselves bona fide geometric phases that are equally valid for pure and mixed states[56] and hence also apply to systems at finite temperature.

Thouless Charge Pumping. A special case of eq 5 occurs when the adiabatic perturbation parametrized by λ is cyclic. In this case, the pumped charge

$$Q = \frac{e}{2\pi} \int_0^1 \mathrm{d}\lambda \int_{-\pi/a}^{\pi/a} \mathrm{d}k \; B_{\lambda k} \tag{15}$$

is a topological invariant.[12,30] We have calculated Q for the cyclic driving protocol $t_1 = t_0 + (t_0/8)\cos(2\pi\lambda)$, $t_2 = t_0 - (t_0/8)\cos(2\pi\lambda)$, and $\Delta = (t_0/8)\sin(2\pi\lambda)$, which pumps charge to the right.[57] A transition from $Q = 2$ to 0 occurs at $U^* = 0.630 \pm 0.001t_0$. An approximate calculation using the reduced Berry curvature

$$B_{\mathrm{red},\lambda k} = 2\,\mathrm{Im} \sum_{n=1}^{\infty} \langle \partial_\lambda v_{nk} | \partial_k v_{nk} \rangle \tag{16}$$

in place of $B_{\lambda k}$ in eq 15 gives an identical transition point $U^* = 0.630 \pm 0.001t_0$. In the case of *nonadiabatic* driving, the pumped charge is no longer quantized, but there is a geometric contribution that can be approximated via the natural orbital geometric phases.[50]

Natural Wannier Functions. The natural Bloch states $|\psi_{n\mathbf{k}}\rangle$ can be used to define natural Wannier functions

$$|w_{n\mathbf{R}}\rangle = \int_{\mathrm{BZ}} \frac{\mathrm{d}^3 k}{(2\pi)^3} e^{-i\mathbf{k}\cdot\mathbf{R}} |\psi_{n\mathbf{k}}\rangle \tag{17}$$

Unlike conventional Wannier functions,[58,59] the $|w_{n\mathbf{R}}\rangle$ are unique (up to trivial relabelings, e.g., due to a shift of origin); the uniqueness of these Wannier functions is a consequence of the gauge-fixing condition for the natural Bloch states $|\psi_{n\mathbf{k}\sigma}\rangle$; correlations provide a "background" that fixes all $\zeta_{n\mathbf{k}}$ up to a gauge transformation of the form $\zeta_{n\mathbf{k}} \rightarrow \zeta_{n\mathbf{k}} + \mathbf{k}\cdot\mathbf{R}_n$, where $\mathbf{R}_n$ is a lattice vector. The Wannier function centers $\langle w_{n0}|\mathbf{r}|w_{n0}\rangle$ correctly give the contribution of each band to the reduced polarization in eq 9, similar to corresponding decompositions for noninteracting electrons.[18,60] Because $\langle w_{n'\mathbf{R}'}|w_{n\mathbf{R}}\rangle = \int \mathrm{d}^3 k \exp[-i\mathbf{k}(\mathbf{R} - \mathbf{R}')] f_{n\mathbf{k}} \delta_{nn'}/(2\pi)^3$, the $|w_{n\mathbf{R}}\rangle$ are not orthonormal and their overlap depends on $f_{n\mathbf{k}}$. More details and examples are available in the Supporting Information.

A different type of natural Wannier function was previously defined[61] in terms of the natural Bloch orbitals $|\phi_{n\mathbf{k}\sigma}\rangle$ without the $(f_{n\mathbf{k}}, \zeta_{n\mathbf{k}})$ information contained in $|\psi_{n\mathbf{k}}\rangle$. Like conventional Wannier functions, the resulting Wannier functions are not unique because making a $\mathbf{k}$-dependent gauge transformation to $|\phi_{n\mathbf{k}\sigma}\rangle$ changes the width and shape of the Wannier functions.

We have found that the reduced information in the natural Bloch states $|\psi_{n\mathbf{k}}\rangle$ contains the most important correlation effects on the macroscopic polarization. The reduced Berry curvature $B_{\mathrm{red},\mu\nu}$ and Berry connection $A_{\mathrm{red},\mu}$ as well as the symmetry properties of the $|\psi_{n\mathbf{k}}\rangle$ states, e.g., under time-reversal and inversion, are promising quantities for practical calculation of topological invariants in the presence of interactions and thermal fluctuations, e.g., in quantum Hall systems,[28,62−64] and topological insulators.[65−69] Our results suggest that replacing the Berry curvature of the full wave function by the reduced Berry curvature will give an accurate approximation to topological invariants. The fact that the $|\psi_{n\mathbf{k}}\rangle$ are built from single-particle orbitals suggests they can be efficiently calculated by ab initio-based methods. This points to the possibility of using the $|\psi_{n\mathbf{k}}\rangle$ states in realistic calculations of topological Mott insulators and other strongly correlated materials for which DFT runs into difficulty.

■ ASSOCIATED CONTENT

Ⓢ Supporting Information

■ AUTHOR INFORMATION

Corresponding Author
*E-mail: rrequist@mpi-halle.mpg.de.
ORCID Ⓞ
Ryan Requist: 0000-0001-6887-3463
Notes
The authors declare no competing financial interest.

■ REFERENCES

(1) Rabe, K., Ahn, C. H., Triscone, J.-M., Eds. *Physics of Ferroelectrics: A Modern Perspective*; Springer-Verlag: Berlin, Heidelberg, 2007.

(2) Grinberg, I.; et al. Perovskite Oxides for Visible-light-absorbing Ferroelectric and Photovoltaic Materials. *Nature* **2013**, *503*, 509.

(3) Frost, J. M.; Butler, K. T.; Brivio, F.; Hendon, C. H.; van Schilfgaarde, M.; Walsh, A. Atomistic Origins of High-Performance in Hybrid Halide Perovskite Solar Cells. *Nano Lett.* **2014**, *14*, 2584.

(4) Yan, W.-L.; Lu, G.-H.; Liu, F. Effect of Chlorine Substitution on Lattice Distortion and Ferroelectricity of CH_3NH_3PbI. *J. Phys. Chem. C* **2016**, *120*, 17972.

(5) Coll, M.; Gomez, A.; Mas-Marza, E.; Almora, O.; Garcia-Belmonte, G.; Campoy-Quiles, M.; Bisquert, J. Polarization Switching and Light-Enhanced Piezoelectricity in Lead Halide Perovskites. *J. Phys. Chem. Lett.* **2015**, *6*, 1408.

(6) Martin, R. M. Comment on Calculations of Electric Polarization in Crystals. *Phys. Rev. B* **1974**, *9*, 1998−1999.

(7) Resta, R. Theory of the Electric Polarization in Crystals. *Ferroelectrics* **1992**, *136*, 51−55.

(8) King-Smith, R. D.; Vanderbilt, D. Theory of Polarization of Crystalline Solids. *Phys. Rev. B: Condens. Matter Mater. Phys.* **1993**, *47*, 1651−1654.

(9) Ortiz, G.; Martin, R. M. Macroscopic Polarization as a Geometric Quantum Phase: Many-body Formulation. *Phys. Rev. B: Condens. Matter Mater. Phys.* **1994**, *49*, 14202−14210.

(10) Resta, R.; Vanderbilt, D. *Theory of Polarization: A Modern Approach*; 2007; pp 31−68; in Ref. 1.

(11) Berry, M. V. Quantal Phase Factors Accompanying Adiabatic Changes. *Proc. R. Soc. London, Ser. A* **1984**, *392*, 45−57.

(12) Thouless, D. J. Quantization of Particle Transport. *Phys. Rev. B: Condens. Matter Mater. Phys.* **1983**, *27*, 6083−6087.

(13) Zak, J. Berry's Phase for Energy Bands in Solids. *Phys. Rev. Lett.* **1989**, *62*, 2747−2750.

(14) Michel, L.; Zak, J. Physical Equivalence of Energy Bands in Solids. *Europhys. Lett.* **1992**, *18*, 239−244.

(15) Resta, R.; Posternak, M.; Baldereschi, A. Towards a Quantum Theory of Polarization in Ferroelectrics: The Case of $KNbO_3$. *Phys. Rev. Lett.* **1993**, *70*, 1010−1013.

(16) Zhong, W.; King-Smith, R. D.; Vanderbilt, D. Giant LO-TO Splittings in Perovskite Ferroelectrics. *Phys. Rev. Lett.* **1994**, *72*, 3618−3621.

(17) Posternak, M.; Baldereschi, A.; Krakauer, H.; Resta, R. Non-Nominal Value of the Dynamical Effective Charge in Alkaline-Earth Oxides. *Phys. Rev. B: Condens. Matter Mater. Phys.* **1997**, *55*, R15983−R15986.

(18) Ghosez, P.; Michenaud, J.-P.; Gonze, X. Dynamical Atomic Charges: the Case of ABO_3 compounds. *Phys. Rev. B: Condens. Matter Mater. Phys.* **1998**, *58*, 6224−6240.

(19) Sághi-Szabó, G.; Cohen, R. E.; Krakauer, H. First-Principles Study of Piezoelectricity in $PbTiO_3$. *Phys. Rev. Lett.* **1998**, *80*, 4321−4324.

(20) Li, Y.; Chen, H.; Huang, L.; Li, J. *Ab Initio* Study of the Dielectric and Electronic Properties of Multilayer GaS Films. *J. Phys. Chem. Lett.* **2015**, *6*, 1059.

(21) Zhang, Y.; Sun, J.; Perdew, J. P.; Wu, X. Comparative First-Principles Studies of Prototypical Ferroelectric Materials by LDA, GGA, and SCAN meta-GGA. *Phys. Rev. B: Condens. Matter Mater. Phys.* **2017**, *96*, No. 035143.

(22) Gonze, X.; Ghosez, P.; Godby, R. W. Density-Polarization Functional Theory of the Response of a Periodic Insulating Solid to an Electric Field. *Phys. Rev. Lett.* **1995**, *74*, 4035−4038.

(23) Godby, R. W.; Needs, R. J. Metal-Insulator Transition in Kohn-Sham Theory and Quasiparticle Theory. *Phys. Rev. Lett.* **1989**, *62*, 1169−1172.

(24) Vignale, G.; Rasolt, M. Density-Functional Theory in Strong Magnetic Fields. *Phys. Rev. Lett.* **1987**, *59*, 2360−2363.

(25) Shi, J.; Vignale, G.; Xiao, D.; Niu, Q. Quantum Theory of Orbital Magnetization and its Generalization to Interacting Systems. *Phys. Rev. Lett.* **2007**, *99*, 197202.

(26) Kohn, W. Theory of the Insulating State. *Phys. Rev.* **1964**, *133*, A171−181.

(27) Laughlin, R. B. Quantum Hall Conductivity in Two Dimensions. *Phys. Rev. B: Condens. Matter Mater. Phys.* **1981**, *23*, 5632−5633.

(28) Thouless, D. J.; Kohmoto, M.; Nightingale, M. P.; den Nijs, M. Quantized Hall Conductance in a Two-Dimensional Periodic Potential. *Phys. Rev. Lett.* **1982**, *49*, 405−408.

(29) Niu, Q.; Thouless, D. J.; Wu, Y.-S. Quantized Hall Conductance as a Topological Invariant. *Phys. Rev. B: Condens. Matter Mater. Phys.* **1985**, *31*, 3372−3377.

(30) Niu, Q.; Thouless, D. J. Quantised Adiabatic Charge Transport in the Presence of Substrate Disorder and Many-Body Interaction. *J. Phys. A: Math. Gen.* **1984**, *17*, 2453−2462.

(31) Löwdin, P.-O. Quantum Theory of Many-Particle Systems. I. Physical Interpretation by Means of Density Matrices, Natural Spin-Orbitals, and Convergence Problems in the Method of Configurational Interaction. *Phys. Rev.* **1955**, *97*, 1474−1489.

(32) Resta, R.; Sorella, S. Many-Body Effects on Polarization and Dynamical Charges in a Partly Covalent Polar Insulator. *Phys. Rev. Lett.* **1995**, *74*, 4738−4741.

(33) Egami, T.; Ishihara, S.; Tachiki, M. Lattice Effect on Strong Electron Correlation: Implication for Ferroelectricity and Superconductivity. *Science* **1993**, *261*, 1307−1310.

(34) Ishihara, S.; Egami, T.; Tachiki, M. Enhancement of the Electron-Lattice Interaction due to Strong Correlation. *Phys. Rev. B: Condens. Matter Mater. Phys.* **1994**, *49*, 8944−8954.

(35) Su, W. P.; Schrieffer, J. R.; Heeger, A. J. Solitons in Polyacetylene. *Phys. Rev. Lett.* **1979**, *42*, 1698−1701.

(36) Rice, M. J.; Mele, E. J. Elementary Excitations of a Linearly Conjugated Diatomic Polymer. *Phys. Rev. Lett.* **1982**, *49*, 1455−1459.

(37) Ortiz, G.; Ordejón, P.; Martin, R. M.; Chiappe, G. Quantum Phase Transitions Involving a Change in Polarization. *Phys. Rev. B: Condens. Matter Mater. Phys.* **1996**, *54*, 13515−13528.

(38) Gidopoulos, N.; Sorella, S.; Tosatti, E. Born Effective Charge Reversal and Metallic Threshold State at a Band Insulator-Mott Insulator Transition. *Eur. Phys. J. B* **2000**, *14*, 217−226.

(39) Carollo, A. C. M.; Pachos, J. K. Geometric Phases and Criticality in Spin-Chain Systems. *Phys. Rev. Lett.* **2005**, *95*, 157203.

(40) Zhu, S.-L. Scaling of Geometric Phases Close to the Quantum Phase Transition in the XY Spin Chain. *Phys. Rev. Lett.* **2006**, *96*, No. 077206.

(41) Cui, H. T.; Yi, J. Geometric Phase and Quantum Phase Transition: Two-Band Model. *Phys. Rev. A: At., Mol., Opt. Phys.* **2008**, *78*, No. 022101.

(42) Yahyavi, M.; Hetényi, B. Reconstruction of the Polarization Distribution of the Rice-Mele Model. *Phys. Rev. A: At., Mol., Opt. Phys.* **2017**, *95*, No. 062104.

(43) Asboth, J. K.; Oroszlany, L.; Palyi, A. *A Short Course on Topological Insulators*; Springer: Cham, Heidelberg, New York, Dordrecht, London, 2016.

(44) Zitko, R. SNEG Mathematica Package for Symbolic Calculations with Second-Quantization-Operator Expressions. *Comput. Phys. Commun.* **2011**, *182*, 2259−2264.

(45) Ben-Israel, A.; Greville, T. N. E. *Generalized Inverses: Theory and Applications*; Springer: New York, 2003.

(46) Requist, R.; Pankratov, O. Time-Dependent Occupation Numbers in Reduced-Density-Matrix-Functional Theory: Application to an Interacting Landau-Zener Model. *Phys. Rev. A: At., Mol., Opt. Phys.* **2011**, *83*, No. 052510.

(47) Coleman, A. J. Structure of Fermion Density Matrices. *Rev. Mod. Phys.* **1963**, *35*, 668−687.

(48) Klyachko, A. A. Quantum Marginal Problem and N-Representability. *J. Phys.: Conf. Ser.* **2006**, *36*, 72−86.

(49) Altunbulak, M.; Klyachko, A. The Pauli Principle Revisited. *Commun. Math. Phys.* **2008**, *282*, 287−322.

(50) Requist, R. Induced Gauge Potentials in Reduced Density Matrix Dynamics. arxiv:1401.3719, 2014.

(51) Löwdin, P.-O.; Shull, H. Natural Orbitals in the Quantum Theory of Two-Electron Systems. *Phys. Rev.* **1956**, *101*, 1730−1739.

(52) Borland, R. E.; Dennis, K. The Conditions on the One-Matrix for Three-Body Fermion Wavefunctions with One-Rank Equal to Six. *J. Phys. B: At. Mol. Phys.* **1972**, *5*, 7−15.

(53) Klyachko, A. The Pauli Exclusion Principle and Beyond. arxiv:0904.2009, 2009.

(54) Schilling, C.; Gross, D.; Christandl, M. Pinning of Fermionic Occupation Numbers. *Phys. Rev. Lett.* **2013**, *110*, No. 040404.

(55) Benavides-Riveros, C. L.; Gracia-Bondía, J. M.; Springborg, M. Quasipinning and Entanglement in the Lithium Isoelectronic Series. *Phys. Rev. A: At., Mol., Opt. Phys.* **2013**, *88*, No. 022508.

(56) Requist, R. Hamiltonian Formulation of Nonequilibrium Quantum Dynamics: Geometric Structure of the Bogoliubov-Born-Green-Kirkwood-Yvon Hierarchy. *Phys. Rev. A: At., Mol., Opt. Phys.* **2012**, *86*, No. 022117.

(57) Vanderbilt, D.; King-Smith, R. D. Electric Polarization as a Bulk Quantity and its Relation to Surface Charge. *Phys. Rev. B: Condens. Matter Mater. Phys.* **1993**, *48*, 4442−4455.

(58) Wannier, G. H. The Structure of Electronic Excitation Levels in Insulating Crystals. *Phys. Rev.* **1937**, *52*, 191−197.

(59) Marzari, N.; Mostofi, A. A.; Yates, J. R.; Souza, I.; Vanderbilt, D. Maximally Localized Wannier Functions: Theory and Applications. *Rev. Mod. Phys.* **2012**, *84*, 1419−1475.

(60) Ghosez, P.; Gonze, X. Band-by-Band Decompositions of the Born Effective Charges. *J. Phys.: Condens. Matter* **2000**, *12*, 9179.

(61) Koch, E.; Goedecker, S. Locality Properties and Wannier Functions for Interacting Systems. *Solid State Commun.* **2001**, *119*, 105.

(62) Avron, J. E.; Seiler, R.; Simon, B. Homotopy and Quantization in Condensed Matter Physics. *Phys. Rev. Lett.* **1983**, *51*, 51.

(63) Kane, C. L.; Mele, E. J. Z_2 Topological Order and the Quantum Spin Hall Effect. *Phys. Rev. Lett.* **2005**, *95*, 146802.

(64) Bernevig, B. A.; Hughes, T. L.; Zhang, S.-C. Quantum Spin Hall Effect and Topological Phase Transition in HgTe Quantum Wells. *Science* **2006**, *314*, 1757.

(65) Fu, L.; Kane, C. L.; Mele, E. J. Topological Insulators in Three Dimensions. *Phys. Rev. Lett.* **2007**, *98*, 106803.

(66) Moore, J. E.; Balents, L. Topological Invariants of Time-Reversal-Invariant Band Structures. *Phys. Rev. B: Condens. Matter Mater. Phys.* **2007**, *75*, 121306.

(67) Roy, R. Topological Phases and the Quantum Spin Hall Effect in Three Dimensions. *Phys. Rev. B: Condens. Matter Mater. Phys.* **2009**, *79*, 195322.

(68) Antonius, G.; Louie, S. G. Temperature-Induced Topological Phase Transitions: Promoted versus Suppressed Nontrivial Topology. *Phys. Rev. Lett.* **2016**, *117*, 246401.

(69) Monserrat, B.; Vanderbilt, D. Temperature Effects in the Band Structure of Topological Insulators. *Phys. Rev. Lett.* **2016**, *117*, 226801.